 doi:10.2136/vzj2012.0046

Field validation of a cosmic-ray neutron sensor using a distributed sensor network

Trenton E. Franz*, M. Zreda*, R. Rosolem*, T.P.A. Ferre*

Abstract

With continued refinement in land surface model resolution the need for accurate and continuous soil moisture datasets at intermediate spatial scales has become critical for improved meteorological and hydrological prediction. The current availability of such data is inadequate. Here, we present a comparison of two datasets that provide average soil moisture over an area hundreds of meters squared in a dryland ecosystem in southern Arizona. One dataset is from a high-resolution soil moisture network of 180 time-domain transmission probes; the other is from a cosmic-ray neutron sensor placed at the center of the study area. We find the cosmic-ray neutron counts correlate well with spatially averaged point measurements of soil moisture over a six-month period with an RMSE of 0.0165 $m^3 m^{-3}$ and percent error of less than 20%. Neutron transport simulations suggest our understanding of the effective sensor depth in the presence of vertical variations in water content is adequate. We find that daily evapotranspiration water fluxes inferred from cosmic-ray measurements agree with previously published eddy-covariance measured values at the study site, suggesting that the cosmic-ray neutron sensor may be able to provide flux measurements of the near surface at intermediate spatial scales.

Trenton E. Franz, M. Zreda, R. Rosolem, and T.P.A. Ferre, Department of Hydrology and Water Resources, University of Arizona, 1133 E James E Rogers Way, Room 122, Tucson, Arizona, 85721 USA; *Corresponding author (tfranz@email.arizona.edu).

doi:10.2136/vzj2012.0046

1. Introduction

As land surface models continue to be refined in space (Wood et al., 2011), the need for high-resolution and high-quality datasets, especially soil moisture, remains critical for validation and calibration of models (Vereecken et al., 2008). While instrumentation and soil moisture sensors have advanced significantly, gaps at different spatial and temporal scales remain, especially intermediate scales (Robinson et al., 2008a; Robinson et al., 2008b), affecting the quality of hydrologic datasets (Binley and Beven, 2003; Day-Lewis and Lane, 2004; Hinnell et al., 2010). A key relationship that needs better understanding is the strength of the land-surface-atmospheric coupling (Koster et al., 2004; Seneviratne et al., 2010), and particularly the need for proper model initialization of soil moisture in order to make accurate weather forecasts. Direct measurements of soil moisture at large spatial scales are difficult, time consuming, and not feasible at many temporal scales or geographic locations. While spaceborne measurements of microwave emissions have satisfied some of the spatial needs, the shallow penetration depth (Njoku et al., 2003) and long repeat times make estimates of accurate soil water fluxes difficult.

The need for continuous long-term measurements of precipitation and soil moisture has been recognized for decades (Manfreda and Rodriguez-Iturbe, 2006; Rodriguez and Mejia, 1974), but because soil moisture is difficult to measure, data at the spatial scale of the continental USA are sparse (Hausman, 2011). However, recent advances in cosmic-ray neutron sensor technology have allowed soil moisture to be quantified continuously in time at intermediate spatial scales (Zreda et al., 2008). A new national network of cosmic-ray soil moisture sensors, the COsmic-ray Soil Moisture Observing System (COSMOS), has recently come online with the goal of improving hydrometeorological forecasting (Zreda et al., 2012), data available at http://cosmos.hwr.arizona.edu/. As part of setting up the national network, a large number of point measurements were made inside the cosmic-ray footprint to calibrate each sensor. We found that collecting 108 samples at 18 different locations inside a 200 m radius circle typically gives reasonable estimates of the mean volumetric water content with a standard error of less than 0.003 m^3 m^{-3}, albeit with a considerable amount of variability. Previous work in Oklahoma and Iowa (Famiglietti et al., 2008) indicate the relationships between different moments of soil moisture averaged over different spatial and temporal scales illustrating the difficulty of capturing area-average soil moisture at intermediate scales from point measurements.

In this work, we compare the results from a network of 180 time-domain transmission probes with a cosmic-ray soil moisture sensor in a highly heterogeneous southern Arizona dryland ecosystem. We compare the spatial average of the point measurements with the cosmic-ray measurements. We next present particle transport modeling results using the observed soil moisture profiles, and finally compute mass balance using the observed cosmic-ray soil moisture values. We conclude with a general discussion on the quality of area-average soil moisture measurements with the cosmic-ray neutron sensor and propose future research directions.

2. Methodology

2.1 Study Site

The field measurements of soil moisture were conducted in the Santa Rita Experimental Range (SRER), approximately 35 km south of Tucson, AZ (Fig. 1a). The

 doi:10.2136/vzj2012.0046

SRER receives an average of ~400 mm of rainfall per year, with 50% occurring between July and September and 30% between December and March (Scott et al., 2008). Daytime temperatures often exceed 35^{o}C in the summer months and 15^{o}C in the winter months. Using eddy covariance techniques, previous studies (Cavanaugh et al., 2011; Scott et al., 2008) calculated actual evapotranspiration rates of 3 to 4 mm day^{-1} in summer months and ~0 to 2 mm day^{-1} during winter months. The study site has ~24% vegetation cover, which is primarily composed of creosotebush (~14%), *Larrea tridentate*, with the remaining vegetation (~10%) composed of grasses, forbes, catci, and mesquite (Cavanaugh et al., 2011). The soils were previously characterized as an Agustin sandy loam with 5 to 15% gravel in the top meter, and having a caliche layer at depths greater than one meter (Cavanaugh et al., 2011). The landscape slopes in a northwest direction with an average angle of 2^{o}. Observations of the surface indicate channelization at the individual plant scale with Hortonian runoff and overland flow leading to redistribution of sediment.

2.2 Soil Moisture Measurements Using a Cosmic-ray Neutron Sensor

A cosmic-ray neutron sensor for quantifying soil moisture (Model CRS-1000 from Hydroinnova LLC, Albuquerque, NM, USA) was installed at the study site on 2 June 2010 as part of the COSMOS network (Zreda et al., 2012). The sensor measures low-energy neutrons (Zreda et al., 2008) and records the total count every hour. Because of the nuclear properties of hydrogen (Glasstone and Edlund, 1952), the relative change in low-energy neutron counts is most correlated to changes in soil water content. Using neutron particle transport modeling, previous studies (Zreda et al., 2008) found that the

 doi:10.2136/vzj2012.0046

sensor has a horizontal support of a circle of approximately 335 m in radius at sea level, and a vertical support of 70 cm in dry conditions and 12 cm at full saturation independent of air pressure. Zreda et al. (2008) defined the support volume as the point at which 86% (i.e. two e-folding or $1-1/e^2$) of the neutrons detected above the surface originated from in the subsurface. Given that fast neutrons travel with velocities > 10 km s^{-1} (Glasstone and Edlund, 1952), the rapid mixing of neutrons (~10^{-4} s, Table 6.147 on page 184 Glasstone and Edlund, 1952) above the heterogeneous surface is practically instantaneous and provides a well-mixed region, which can effectively be sampled with a point detector. In addition, the average collision free path (distance between successive collisions) of a neutron traveling in air is ~30 m with tens of collisions occurring between the creation of low-energy neutrons (~10^6 eV) and eventual thermalization or detection of those neutrons (~10^1 to 10^2 eV) used for soil moisture measurements (Desilets et al., 2010). By comparing the collision free path length and horizontal scale of soil moisture organization, we assume that horizontal heterogeneity at most natural sites will not be important as the length scale of soil moisture correlation is much smaller than 30 m. We note that this has yet to be fully validated with experimental or modeling results and remains an open research question.

Using a neutron particle transport model, Desilets et al. (2010) found a theoretical relationship between relative neutron counts and soil water content in homogeneous sand (SiO_2):

$$\theta(N) = \frac{0.0808}{\left(\frac{N}{N_0}\right) - 0.372} - 0.115 \qquad (1)$$

where θ (m^3 m^{-3}) is the average volumetric water content, N is the neutron counting rate (count hr^{-1}) normalized to a reference atmospheric pressure and solar activity level, and N_0 (count hr^{-1}) is the counting rate over dry soil under the same reference conditions and needs to be estimated with at least one independent soil moisture calibration. Full details on the correction factors for variations in atmospheric pressure and geomagnetic latitude (Desilets and Zreda, 2003), and solar activity level (Zreda et al., 2012) are discussed elsewhere. We note that these correction factors are automated on the COSMOS website with full hourly details provided in data levels 1 and 2.

Because neutrons are affected by all sources of hydrogen in the support volume, we have included an additional neutron correction factor for variations in atmospheric water vapor (Zreda et al., 2012). Rosolem et al. (In Review) found a water vapor correction factor, C_{WV}, using a neutron particle transport model:

$$C_{WV} = 1 + 0.0054\left(\rho_v^0 - \rho_v^{ref}\right) \quad (2)$$

where ρ_v^0 (g m^{-3}) is the average density of air in a ~335 m radius hemisphere above the surface, and ρ_v^{ref} (g m^{-3}) is the average density of air at a reference condition. Estimates of average air density can be made with surface measurements of air temperature, air pressure, relative humidity, and assuming standard atmospheric lapse rates. We note that at SRER that water vapor greatly varies between the dry and wet season resulting in neutron correction factors up to 5 to 10% at the extremes.

In order to estimate the free parameter N_0 in equation (1), we performed five different soil moisture calibration datasets. Volumetric samples were collected at 18 locations (every 60 degrees from 0 to 360 and at radial distances of 25, 75, and 200 m along each transect) and at 6 depths (0-5, 5-10, 10-15, 15-20, 20-25, 25-30 cm) for a total

 doi:10.2136/vzj2012.0046

of 108 samples. Given the radial sensitivity of the cosmic-ray sensor, every location is given equal weight in an estimate of area-average soil moisture. Figure 1 illustrates two horizontal cumulative sensitivity contours at SRER for the cosmic-ray neutron sensor. Note that the 63% (one e-folding) and 86% (two e-folding) contours are 10% larger than previously reported (Zreda et al., 2008), as air density at SRER (elevation 989 m) is ~10% less than at sea level, thus allowing neutrons to travel farther. The volumetric soil samples were collected in a 30 cm long split tube corer with 5.08 cm diameter sample rings (Model 355.42 from AMS Inc., American Falls, ID, USA). The gravimetric weight loss was recorded in each sample following oven drying at 105^{o}C for 48 hours and attributed to pore water (Dane and Topp, 2002). We note at SRER that it took approximately 6 hours to collect a full calibration dataset and therefore took a six-hour average neutron count, N, over the same period in order to determine N_0 in equation (1).

2.3 Soil Moisture Measurements Using a Distributed Sensor Network

In the same general pattern as the volumetric calibration datasets, profiles of time-domain transmission probes (TDT) (Model ACC-SEN-TDT from Acclima Inc., Meridian, ID, USA) were installed between 15 and 26 June 2011 (Fig. 1). Acclima TDT probes have been shown to have performance equivalent to conventional TDR (Blonquist et al., 2005b). At each site, probes were placed horizontally at 10, 20, 30, 50, and 70 cm both in open areas and beneath a creosotebush within 3 meters of each other for a paired study. Following excavation of a 1 m^3 soil pit, a chisel of the same dimensions as the TDT probe was used to excavate a cavity in the upslope soil face. The TDT probe was then placed in the cavity using the excavated soil to backfill the remaining void space.

After all five probes were in place; we repacked the excavated soil pit using the soil from the same depth location. A tipping bucket rain gauge was also installed at each location (Model TE525m from Campbell Scientific Inc., Logan, UT, USA). Data was recorded every 30 minutes for each TDT probe and individual tips (0.1 mm) were recorded for each rain gage.

Before their deployment in the field, the TDT probes were calibrated in a laboratory by using four substances with a range of dielectric permittivities (Fig. 2), following procedures outlined in (Kelleners et al., 2005). The observed volumetric water contents indicate normally distributed behavior around a mean with standard deviations of 0.01 to 0.02 m^3 m^{-3} for each medium, with error levels consistent with previous studies (Blonquist et al., 2005a; Topp et al., 1980). In addition, the individual profiles were calibrated in the field during two different volumetric calibration datasets, 11 September 2011 and 15 December 2011. The comparison between the volumetric samples and the TDT probes (manufacturer provided mixing model) indicated a mean bias of 0.02 m^3 m^{-3} overestimate of soil moisture by the probe in the SRER soils over the top 30 cm. The bias was consistent for all TDT probes at 10, 20, and 30 cm with comparisons of the volumetric samples averaged over 5-15 cm, 15-25 cm, and 25-30 cm, collected from the same relative locations during the two volumetric calibration datasets. Given the destructive nature of volumetric sampling, we note that we were not able to sample at the exact same location and that the bias may be due to horizontal variability at the site or due to the implicit uncertainties resulting from repacking soil around the in-situ probes. Over the course of the experiment, 160 TDT probes (out of 180 installed) and 12 rain gages (out of 18 installed) worked continuously without any noticeable problems or

 doi:10.2136/vzj2012.0046

systematic drift. Given the relatively low soil moisture values and large soil temperature transients, the in-situ TDT probes performed well with ~90% data success rate. In order to compare the soil moisture from the cosmic-ray neutron sensor and the TDT probes, we assume a -0.02 m^3 m^{-3} bias correction for all TDT probes, based on the volumetric calibration of the TDT probes.

2.4 Depth Weighting of Soil Moisture Measurements

In order to compare the area-average soil moisture values from the cosmic-ray neutron sensor and the volumetric and TDT measurements we needed to average the point measurements in a compatible manner. The horizontal locations of the point measurements were selected (Fig. 1b) such that each point, representative of the area, had equal horizontal weight. We therefore took an arithmetic average of each point measurement by depth. More complex is the vertical depth averaging given the moving vertical support of the cosmic-ray sensor (Zreda et al., 2008). The effective depth of the sensor varies with water content, lattice water, and soil dry bulk density. Using a neutron particle transport model, Franz *et al.* (In Review) estimated the 86% (i.e. two e-folding) cumulative depth sensitivity contour, φ (cm), from three homogeneous cases (dry sand, wet sand, liquid water):

$$\varphi(z) = 5.8 - 0.0829z \quad 0 \le z \le 70 \tag{3}$$

where z is the vertical distance in the soil (cm), 5.8 (cm) represents the 86% cumulative sensitivity depth of low-energy neutrons in liquid water, and the slope of the relationship (0.0829) is controlled by the nuclear cross sections of SiO_2.

 doi:10.2136/vzj2012.0046

In order to compute an effective sensor depth, it was assumed that the effective sensor depth was the point at which the sum of water, *LW* (cm), from surface W_S (cm), pore W_P (cm), and lattice water W_L (cm) sources crosses the 86% cumulative sensitivity contour given by equation (3). The sum of water as a function of soil depth from the three different sources is:

$$LW(z) = W_s + \frac{\rho_{bd}(z)\tau(z)z}{\rho_w} + \theta(z)z \qquad (4)$$

where ρ_{bd} is the dry bulk density of soil (g cm^{-3}), ρ_w is the density of liquid water (g cm^{-3}), and τ is the weight fraction of lattice water in the mineral grains and bound water, defined as the amount of water released at 1000^{o}C detected using infrared methods and preceded by drying at 105^{o}C (g of water per g of dry minerals, herein known as lattice water, test specifics available at http://www.actlabs.com/page.aspx?page=530&app=226&cat1=549&tp=12&lk=no&menu=64, Table 1). By setting equation (3) equal to the integral of equation (4) we are able to define a general relationship for the effective sensor depth, *z** (cm):

$$\phi(z^*) = W_s + \int_0^{z^*} \left(\frac{\rho_{bd}(z)\tau(z)}{\rho_w} + \theta(z) \right) dz \qquad (5)$$

For uniform distributions of bulk density, pore water, and lattice water, equation (5) simplifies to a closed solution for *z**:

$$z^* = \frac{5.8}{\frac{\rho_{bd}}{\rho_w}\tau + \theta + 0.0829} \qquad (6)$$

where ρ_w is assumed to be 1 g cm^{-3}.

With the effective sensor depth defined, a simple linear depth weighting function, *wt*, is proposed as a function of soil depth:

$$\begin{cases} wt(z) = a\left(1-\left(\frac{z}{z^*}\right)\right) & 0 \le z \le z^* \\ wt(z) = 0 & z > z^* \end{cases} \tag{7}$$

where *a* is a constant defined by the condition that the weights are conserved, $1 = \int_0^{z^*} a\left(1-\left(\frac{z}{z^*}\right)\right)dz$, which yields the solution $a = \frac{1}{z^* - \frac{z^{*2}}{2z^*}}$. Desilets (unpublished data) has developed a depth weighting function based on nuclear cross sections, where the functional form is a product of exponentials representing the production and absorption of neutrons in dry and wet soil layers. Preliminary results indicate the linear depth weighting function presented here is a reasonable first order approximation for a range of soil moisture profiles and given its simplicity it is adopted in this analysis.

For the remaining analyses we use equations (5) and (7) to compute depth-weighted profiles of the volumetric and TDT calibration/validation datasets, assuming W_S is 0 for all cases. Using equation (6), the effective depth of the cosmic-ray sensor time series at SRER varies between 20 cm and 40 cm throughout.

2.5 Neutron Transport Particle Modeling

We used the 3-dimensional Monte Carlo N-Particle eXtended model (MCNPx) (Pelowitz, 2005) to simulate the transport of cosmic-ray particles throughout the atmosphere and near the surface over low to medium energy levels (0 to ~200GeV). MCNPx is general purpose Monte Carlo model that simulates the life history of an individual particle and its consequent particles as it interacts with different elements in the atmosphere and near surface. The simulations used the same particle source function,

 doi:10.2136/vzj2012.0046

domain, and neutron detector as those in previous work (Zreda et al., 2008), but used the latest cross section libraries provided by the MCNPx user community. We use horizontally averaged layers and include only vertical heterogeneities in the domain. Unlike previous work (Zreda et al., 2012), we used the local soil chemistry and dry bulk density observed at SRER (Table 1). Table 1 shows the weight percent of 14 major rock-forming elements from samples collected at SRER that make up over 99% of the mass of the material (soils analyzed at Actlabs, Ancaster, Ontario, Canada). In agreement with previous work (Zreda et al., 2008), we found that modeled fast neutron flux (~10 to 100eV) is weakly correlated to parent material because hydrogen dominates neutron scattering (Zreda et al., 2012) (Fig. 3b). However, we note that hydrogen in the mineral structure of soil (a.k.a. lattice water or H_2O^+, defined as τ in section 2.4) can significantly differ among soil types (Greacen, 1981). Therefore, the relationship between fast neutrons and volumetric water content in the pore space may be affected, (Fig. 3a), requiring slight modifications to the coefficients in equation (1) (Desilets et al., 2010), that may not be accounted for explicitly in the N_0 parameter. We note that the variation is most likely strongest at the dry end, where lattice water can account for a majority of the hydrogen present in the sensor support volume.

3. Results

3.1 Distributed Sensor Network

The half hourly time series of the paired profiles indicates a significant amount of soil moisture variability in the top 30 cm around the footprint (Fig. 4). Not surprisingly, the paired profiles illustrate that soil moisture dynamics can be nearly identical (Fig. 4a

 doi:10.2136/vzj2012.0046

versus 4b), similar (Fig. 4c versus 4d), or different (Fig. 4e versus 4f). We found that peak soil moisture following precipitation events was slightly higher on average in canopy profiles compared to open profiles (~0.02 $m^3 m^{-3}$). We also found that no wetting fronts reached the 50 cm probes during the summer monsoons. However, rainfall events in the winter season, when evapotranspiration is lower, led to deep percolation around the footprint as indicated by both the individual profiles (Fig. 4, particularly 4a and 4d) and the spatially averaged TDT profiles at 50 and 70 cm (Fig. 5), which is consistent with previous work (Scott et al., 2000). The spatial average of the TDT probes results in a standard error of the mean of less than 0.01 $m^3 m^{-3}$ for all depth profiles (Fig. 5a). The standard error of daily rainfall from 12 gauges is ~2-3 mm for a range of rainfall totals (Fig. 5b). A summary of the hourly TDT profiles and daily rainfall is provided at http://cosmos.hwr.arizona.edu/Probes/StationDat/011/index.php.

3.2 Comparison of Area-Average Soil Moisture Datasets

To compare the volumetric and TDT soil moisture calibration/validation datasets with the cosmic-ray neutron data we computed the depth weighted water content over a six hour period using equations (5) and (7), which is the typical length of time required to collect a full volumetric calibration dataset. With the longer integration time we note that this will reduce the neutron count rate uncertainty (Zreda et al., 2008) from approximately 44 counts hr^{-1} to 18 counts hr^{-1} for a typically SRER count rate of 2000 counts hr^{-1}. Table 2 summarizes the five volumetric calibration datasets collected at the study site. The average neutron counts are corrected for variations in pressure, geomagnetic latitude, and neutron intensity as summarized in section 2.2 and implemented in data Levels 1 and 2 on the COSMOS website, http://cosmos.hwr.arizona.edu/Probes/StationDat/011/index.php. In addition, we corrected for variations in hourly atmospheric water vapor by using continuous measurements of air temperature, air pressure, and relative humidity described in equation (2). The same procedure was used for 6 hour periods of data from the TDT validation datasets with data available at http://cosmos.hwr.arizona.edu/Probes/StationDat/011/index.php.

The computed N_0 values using equation (1), from the five different volumetric calibration datasets are summarized in Table 3. We found that N_0 varied between 3311 and 3116 counts hr^{-1} between the five different datasets. Comparison of the various values indicated a maximum soil moisture deviation of 0.0295 m^3 m^{-3} between all datasets, with average deviations less than 0.017 m^3 m^{-3}. Using all five volumetric calibration datasets we found a best fit N_0 of 3187 with an $R^2 = 0.927$, RMSE = 0.00953 m^3 m^{-3} and $p < 0.001$. The best fit N_0 resulted in an average deviation of 0.0097 m^3 m^{-3} between all calibration datasets and a percent error of 19.4% at 0.05 m^3 m^{-3} and 6.5% at 0.15 m^3 m^{-3}.

Using the best fit N_0 from the volumetric calibration datasets, Figure 6 illustrates the relationships between the derived calibration function, equation (1) with $N_0 = 3187$ counts hr^{-1}, the five volumetric calibration datasets and the continuous TDT validation datasets over the study period. Using the derived calibration function, we find the TDT validation datasets have an $R^2 = 0.822$, RMSE = 0.0165 m^3 m^{-3} and $p < 0.001$ over the 6-month study period. The remaining 18.8% of variation in the signal is likely due to a variety of reasons including: neutron count uncertainty (Zreda et al., 2008; Zreda et al.,

 doi:10.2136/vzj2012.0046

2012), sampling uncertainty and spatial variability, slight hysteresis in neutron counts during wetting and drying fronts, and changes in background hydrogen pools other than those considered in the analysis. Overall the RMSE of 0.0165 $m^3 m^{-3}$ is small, and well within the uncertainty observed in the TDT laboratory calibration (Fig. 2) and reported in the TDT literature (Blonquist et al., 2005b), and in the volumetric calibration datasets (Table 2).

We used MCNPx to compute the average water content that the cosmic-ray sensor would see given the distribution of pore water from the observed TDT profiles. The comparison between the computed TDT weighted average value and MCNPx modeled value (Fig. 7a) shows an RMSE of 0.0044 $m^3 m^{-3}$, with maximum deviations of 0.01 to 0.02 $m^3 m^{-3}$ during high near-surface soil moisture due to the existence of sharp wetting fronts in the profile. Using the calibration function estimated in Figure 6, we can compare the cosmic-ray soil moisture data with the TDT weighted averaged values (Fig. 7b). We find a RMSE of 0.0108 $m^3 m^{-3}$, and maximum deviation of 0.03 to 0.04 $m^3 m^{-3}$ during high near-surface soil moisture periods. In addition, we find that the cosmic-ray soil moisture time series decays faster during dry-down periods and is more responsive to small rain events (< 5 mm), which is discussed in more detail in section 4.2.

3.3 Cosmic-Ray Sensor Mass Balance

As an additional confirmation of the quality of geophysical datasets (Huisman et al., 2001), we compute the daily and total water mass balance using only the cosmic-ray soil moisture time series and rainfall (Fig. 8 and Table 4). In order to compute a daily flux, we first subtract the daily average soil moisture values and then multipy by the

 doi:10.2136/vzj2012.0046

minimum value of the two effective sensor depth estimates. By working with daily average values, we smooth the soil moisture time series and may underestimate the total flux. In the daily soil water fluxes (Fig 8a), positive values indicate periods of net inflow into the footprint due to infiltration, and negative values represent net outflow due to evapotranspiration and deep drainage. The daily time series of negative fluxes indicate maximum observed evapotranspiration of 3 to 4 mm day^{-1} in the summer months and 1 to 2 mm day^{-1} in the winter, which is consistent with eddy covariance data observed at this site (Cavanaugh et al., 2011; Scott et al., 2008). By comparing the daily value of infiltration and rainfall we find that runoff ratios (assuming rainfall interception loss is less than 1 mm and negligible) vary between ~0 for small rain events and 0.5 for the largest 45 mm rain event. The total seasonal water balance indicates runoff around 20%, 5% for change in seasonal storage, and 75% for evapotranspiration and deep drainage (Table 4). Preliminary analysis of the sensor data indicates it conserves mass at the daily and seasonal time scales, but additional future datasets such as full eddy covariance and runoff should be analyzed for fuller confirmation.

4. Discussion

4.1 Quality of Area-Average Soil Moisture Measurements With Cosmic-ray Neutron Sensors

Despite large spatial variability between individual soil moisture TDT profiles (Fig. 4), we found that measurements of above ground low-energy neutrons accurately capture the mean soil moisture behavior (Fig. 7). By using several volumetric calibration datasets to define the N_0 parameter in equation (1), we found good agreement (R^2 =

0.822) with independent continuous area-average measurements using a distributed sensor network (Fig. 6). With one independent volumetric calibration dataset we found that the average absolute deviation between calibration datasets was less than 0.017 m^3 m^{-3} with a percent error on the order of 20% or less (Table 3). As with most sensors, we found that multiple calibration datasets across the range of variability will lead to the highest confidence in measurements with an RMSE ~0.0165 m^3 m^{-3}, which is within the reported uncertainty for TDT probes (Blonquist et al., 2005b).

As good practice for data quality and assurance of cosmic-ray neutron sensors we recommend the following procedures in addition to the standard pressure, geomagnetic latitude, and neutron intensity corrections: 1) at least one volumetric calibration dataset to determine N_0, with additional calibration datasets preferred, 2) continuous measurements of air temperature, air pressure, and relative humidity to account for temporal variations in water vapor 3) one estimate of mineral lattice water for use in estimating effective sensor depth and thus estimating depth weighted averages from discrete point measurements. As an additional source of calibration standards and procedures, methods developed using the in-situ neutron probe may be helpful (Bell, September 1987; Greacen, 1981; Visvalingam and Tandy, 1972). In particular, the method developed in France by the Commissariate a l'Energie Atomique utilizes direct measurements of the macroscopic nuclear cross-sections from field samples in an atomic pile in order to establish a local calibration functio. We note that the cosmic-ray neutron sensor uses fast neutrons (~10^1 to 10^2eV) as compared to the in-situ neutron probe that uses thermal neutrons (<0.025eV) to quantify soil moisture. This means that the cosmic-ray neutron

 doi:10.2136/vzj2012.0046

sensor will be less sensitive to local soil chemistry variations like Boron or Gadolinium (Zreda et al., 2008, Table S1).

As an active area of research, it may be important to account for other site-specific transient hydrogen sources that may affect neutron counts, such as fast growing vegetation like corn (Hornbuckle et al., 2011). We note that static background hydrogen sources will be implicitly accounted for in the N_0 estimation but any time-varying hydrogen sources may need to be considered. As stated previously (Bell, September 1987), it is the relative differences in neutron counts at a site that are key to determining the time-varying change of hydrogen, most notably soil water content.

4.2 Sensitivity to Shallow Layer Dynamics

Comparisons between the cosmic-ray soil moisture and TDT weighted averages indicate two systematic differences between the two signals: one is the higher sensitivity of neutron counts to small rain events, the other is the faster decay of the neutron signal during dry-down periods (Fig. 7b). Equation (7) quantifies the decreasing sensitivity of the cosmic-ray sensor with soil depth, as relatively more neutrons escape from shallower zones than deeper zones. The reason for both deviations lies not in the nature of the two systems, but in our inability to adequately capture the shallow (0-10 cm) layer dynamics because the shallowest TDT probe was placed horizontally at 10 cm depth. Given that surface water redistribution occurs at the study site, we chose to insert the probes horizontally instead of vertically through the surface to prevent potential preferential flow pathways. As a consequence, we do not record changes in soil moisture that occur in the top 5 cm. In addition, the top layer will dry out faster than the recorded values given by

doi:10.2136/vzj2012.0046

the 10 cm probes due to the high potential evaporation at the study site resulting in the steeper slope recorded by the cosmic-ray sensor during dry-down periods.

While our lack of direct water content measurements in the uppermost 10 cm presents some limitations to our study, it also suggests a potential advantage of cosmic-ray measurements. Specifically, given the high sensitivity of cosmic-ray measurements to the shallow subsurface, cosmic-ray datasets may have great potential for validating passive microwave sensors given their penetration depths of centimeters (Jackson et al., 1997). This will be tested in the near future using cosmic-ray sensors that are co-located at SMOS Cal/Val sites (Zreda et al., August 2011).

5. Conclusions

In this work we have shown that independent continuous measurements of soil moisture from a network of TDT probes compare well with a cosmic-ray neutron sensor calibrated with volumetric soil moisture samples. Moreover, we have found that cosmic-ray sensor soil moisture data provide reasonable estimates of water flux and conserve mass at daily and seasonal timescales for water limited, dryland ecosystems where rainfall penetrates to limited depth, suggesting our understanding of effective sensor depth for the cosmic-ray sensor may be adequate. Based on these results, we suggest that further research should investigate the cosmic-ray based measurements of soil moisture for different soil types, differing hydrological regimes, with the potential to infer soil moisture and water flux, at intermediate spatial scales helping calibrate and validate land surface models for improved weather prediction, validating remote sensing products and potential to aid irrigation management.

Acknowledgements

This research and the COSMOS project were supported by the US National Science Foundation grant AGS-0838491. We would like to thank the management of the Santa Rita Experimental Range for the permission to conduct the research there. We also thank Jim Shuttleworth, Xubin Zeng, Shirley Papuga, Adam Karczynski, Bobby Chrisman, Susan Stillman, Chris Zweck, Darin Desilets, Gary Womack, Hydroinnova, Quaesta Instruments, and Acclima for their support and help with different aspects of the work. We would also like to thank David Robinson, Scott Jones, and two anonymous reviewers for their helpful comments.

References

Bell, J. P. (September 1987), Neutron Probe Practice. Report 19, Insittue of Hydrology.

Binley, A., and K. Beven. 2003. Vadose zone flow model uncertainty as conditioned on geophysical data. Ground Water 41:2: 119-127.

Blonquist, J. M., S. B. Jones, and D. A. Robinson. 2005a. Standardizing characterization of electromagnetic water content sensors: Part 2. Evaluation of seven sensing systems. Vadose Zone Journal 4:4: 1059-1069. doi:10.2136/vzj2004.0141.

Blonquist, J. M., S. B. Jones, and D. A. Robinson. 2005b. A time domain transmission sensor with TDR performance characteristics. Journal of Hydrology 314:1-4: 235-245. doi:10.1016/j.jhydrol.2005.04.005.

Cavanaugh, M. L., S. A. Kurc, and R. L. Scott. 2011. Evapotranspiration partitioning in semiarid shrubland ecosystems: a two-site evaluation of soil moisture control on transpiration. Ecohydrology 4:5: 671-681. doi:10.1002/eco.157.

Dane, J. H., and C. G. Topp. 2002. Methods of Soil Analysis: Part 4 Physical Methods. Soil Science Society of America. Madison, WI.

Day-Lewis, F. D., and J. W. Lane. 2004. Assessing the resolution-dependent utility of tomograms for geostatistics. Geophysical Research Letters 31:7: 4. doi:L07503 10.1029/2004gl019617.

Desilets, D., and M. Zreda. 2003. Spatial and temporal distribution of secondary cosmic-ray nucleon intensities and applications to in situ cosmogenic dating. Earth and Planetary Science Letters 206:1-2: 21-42. doi:10.1016/s0012-821x(02)01088-9.

Desilets, D., M. Zreda, and T. P. A. Ferre. 2010. Nature's neutron probe: Land surface hydrology at an elusive scale with cosmic rays. Water Resources Research 46. doi:W11505 10.1029/2009wr008726.

Famiglietti, J. S., D. R. Ryu, A. A. Berg, M. Rodell, and T. J. Jackson. 2008. Field observations of soil moisture variability across scales. Water Resources Research 44:1: 16. doi:W01423 10.1029/2006wr005804.

Franz, T. E., M. Zreda, P. A. Ferre, R. Rosolem, C. Zweck, S. Stillman, X. Zeng, and W. J. Shuttleworth (In Review), Measurement depth of the cosmic-ray soil moisture probe affected by hydrogen from various sources, *Water Resources Research*.

Glasstone, S., and M. C. Edlund. 1952. Elements of Nuclear Reactor Theory. Van Nostrand. New York.

Greacen, E. L. (1981), Soil Water Assessment by the Neutron Method, CSIRO, Melbourne.

Hausman, S. A. (2011), USCRN Annual Report for FY 2011.

Hinnell, A. C., T. P. A. Ferré, J. A. Vrugt, J. A. Huisman, S. Moysey, J. Rings, and M. B. Kowalsky. 2010. Improved extraction of hydrologic information from geophysical data through coupled hydrogeophysical inversion. Water Resources Research 46: 14.

Hornbuckle, G., S. Irvin, and J. Patton. 2011. Impact of Rapidly Growing Vegetation On COSMOS Measurements. Abstract 243-4 presented at 2011 ASA, CSSA, SSSA Annual Meeting, San Antonio, Texas, 16-19 Oct.

Huisman, J. A., C. Sperl, W. Bouten, and J. M. Verstraten. 2001. Soil water content measurements at different scales: accuracy of time domain reflectometry and ground-penetrating radar. Journal of Hydrology 245:1-4: 48-58. doi:10.1016/s0022-1694(01)00336-5.

Jackson, T. J., P. E. Oneill, and C. T. Swift. 1997. Passive microwave observation of diurnal surface soil moisture. IEEE Trans. Geosci. Remote Sensing 35:5: 1210-1222. doi:10.1109/36.628788.

Kelleners, T. J., M. S. Seyfried, J. M. Blonquist, J. Bilskie, and D. G. Chandler. 2005. Improved interpretation of water content reflectometer measurements in soils. Soil Sci. Soc. Am. J. 69:6: 1684-1690.

Koster, R. D., P. A. Dirmeyer, Z. C. Guo, G. Bonan, E. Chan, P. Cox, C. T. Gordon, S. Kanae, E. Kowalczyk, D. Lawrence, P. Liu, C. H. Lu, S. Malyshev, B. McAvaney, K. Mitchell, D. Mocko, T. Oki, K. Oleson, A. Pitman, Y. C. Sud, C. M. Taylor, D. Verseghy, R. Vasic, Y. K. Xue, T. Yamada, and G. Team. 2004. Regions of strong coupling between soil moisture and precipitation. Science 305:5687: 1138-1140. doi:10.1126/science.1100217.

Manfreda, S., and I. Rodriguez-Iturbe. 2006. On the spatial and temporal sampling of soil moisture fields. Water Resources Research 42:5: 10. doi:W05409 10.1029/2005wr004548.

Njoku, E. G., T. J. Jackson, V. Lakshmi, T. K. Chan, and S. V. Nghiem. 2003. Soil moisture retrieval from AMSR-E. IEEE Trans. Geosci. Remote Sensing 41:2: 215-229. doi:10.1109/tgrs.2002.808243.

Pelowitz, D. B. (Ed.) (2005), *MCNPX user's manual, version 5, Rep. LA-CP-05-0369*, Los Alamos National Laboratory, Los Alamos.

Robinson, D. A., A. Binley, N. Crook, F. D. Day-Lewis, T. P. A. Ferre, V. J. S. Grauch, R. Knight, M. Knoll, V. Lakshmi, R. Miller, J. Nyquist, L. Pellerin, K. Singha, and L. Slater. 2008a. Advancing process-based watershed hydrological research using near-surface geophysics: a vision for, and review of, electrical and magnetic geophysical methods. Hydrological Processes 22:18: 3604-3635.

Robinson, D. A., C. S. Campbell, J. W. Hopmans, B. K. Hornbuckle, S. B. Jones, R. Knight, F. Ogden, J. Selker, and O. Wendroth. 2008b. Soil moisture measurement for ecological and hydrological watershed-scale observatories: A review. Vadose Zone Journal 7:1: 358-389.

Rodriguez, I., and J. M. Mejia. 1974. Design of rainfall networks in time and space. Water Resources Research 10:4: 713-728. doi:10.1029/WR010i004p00713.

Rosolem, R., W. J. Shuttleworth, M. Zreda, T. E. Franz, and X. Zeng (In Review), The Effect of Atmospheric Water Vapor on the Cosmic-ray Soil Moisture Signal, J. Hydrometeorol.

Scott, R. L., W. J. Shuttleworth, T. O. Keefer, and A. W. Warrick. 2000. Modeling multiyear observations of soil moisture recharge in the semiarid American Southwest. Water Resources Research 36:8: 2233-2247. doi:10.1029/2000wr900116.

Scott, R. L., W. L. Cable, and K. R. Hultine. 2008. The ecohydrologic significance of hydraulic redistribution in a semiarid savanna. Water Resources Research 44:2: 12. doi:W02440
10.1029/2007wr006149.

Seneviratne, S. I., T. Corti, E. L. Davin, M. Hirschi, E. B. Jaeger, I. Lehner, B. Orlowsky, and A. J. Teuling. 2010. Investigating soil moisture-climate interactions in a changing climate: A review. Earth-Science Reviews 99:3-4: 125-161. doi:10.1016/j.earscirev.2010.02.004.

Topp, G. C., J. L. Davis, and A. P. Annan. 1980. Electromagnetic Determination of Soil-Water Content - Measurements in Coaxial Transmission-Lines. Water Resources Research 16:3: 574-582.

Vereecken, H., J. A. Huisman, H. Bogena, J. Vanderborght, J. A. Vrugt, and J. W. Hopmans. 2008. On the value of soil moisture measurements in vadose zone hydrology: A review. Water Resources Research 44. doi:W00d06 10.1029/2008wr006829.

Visvalingam, M., and J. D. Tandy. 1972. Neutron Method For Measuring Soil-Moisture Content- Review. Journal of Soil Science 23:4: 499-511.

Wood, E. F., J. K. Roundy, T. J. Troy, L. P. H. van Beek, M. F. P. Bierkens, E. Blyth, A. de Roo, P. Doll, M. Ek, J. Famiglietti, D. Gochis, N. van de Giesen, P. Houser, P. R. Jaffe, S. Kollet, B. Lehner, D. P. Lettenmaier, C. Peters-Lidard, M. Sivapalan, J. Sheffield, A. Wade, and P. Whitehead. 2011. Hyperresolution global land surface modeling: Meeting a grand challenge for monitoring Earth's terrestrial water. Water Resources Research 47: 10. doi:W05301 10.1029/2010wr010090.

Zreda, M., D. Desilets, T. P. A. Ferre, and R. L. Scott. 2008. Measuring soil moisture content non-invasively at intermediate spatial scale using cosmic-ray neutrons. Geophysical Research Letters 35:21: 5. doi:L21402 10.1029/2008gl035655.

Zreda, M., W. J. Shuttleworth, X. Xeng, C. Zweck, D. Desilets, T. E. Franz, R. Rosolem, and P. A. Ferre. 2012. COSMOS: The COsmic-ray Soil Moisture Observing System.

Hydrology and Earth System Sciences Disscussion 9: 4505-4551. doi:10.5194/hessd-9-4505-2012.

Zreda, M., X. Zeng, S. W.J., C. Zweck, P. A. Ferre, T. E. Franz, R. Rosolem, D. Desilets, S. Desilets, and G. Womack. August 2011. Cosmic-Ray Neutrons, An Innovative Method for Measuring Area-Average Soil Moisture. GEWEX News 21:3.

 doi:10.2136/vzj2012.0046

Figure Captions

Figure 1. a) Location and two radial cumulative sensitivity contours of the cosmic-ray soil moisture sensor at Santa Rita Experimental Range in Southern Arizona (31.9085^{o}N 110.8394^{o}W, elevation 989 m). b) Location of eighteen paired soil moisture profiles in open areas and below the canopy where TDT probes were inserted horizontally at 10, 20, 30, 50, and 70 cm depths. Letters a-f are keyed to profiles illustrated in Figure 4. Satellite image is from Google Earth.

Figure 2. Response of 170 TDT probes used in the experiment when submerged in four different media with varying permittivity: a) air dried soil from SRER, b) isopropyl alcohol, c) fully saturated clean sand, and d) deionized water.

Figure 3. a) The MCNPx modeled fast neutron flux versus pore water content for SiO_2 and SRER soil chemistries. b) The two modeled datasets collapse to nearly the same curve when summing total water from both lattice and pore water soil pools.

Figure 4. Time series of three paired TDT profiles (a-b, c-d, e-f) at different locations (shown in Fig. 1b) within the cosmic-ray footprint. Left column: profiles in open areas, right column: profiles under canopy.

Figure 5. a) Time series of spatially averaged TDT water content by depth and weighted average from eighteen paired profiles. b) Time series of daily rainfall from twelve rain

 doi:10.2136/vzj2012.0046

gauges within footprint. Error bars are 1 standard error of the mean. Weighted averages are computed from equations (5) and (7).

Figure 6. Relationship between observed fast neutron counts and five different volumetric calibration datasets and continuous TDT validation datasets. Data points are averaged over 6 hours periods and weighted by depth with equations (5) and (7). Fitted curves are significant at $p < 0.001$ level.

Figure 7. a) Comparison between TDT weighted average water content and MCNPx modeled water content using observed spatially averaged profiles from 10, 20, 30, 50, and 70 cm. b) Comparison between TDT weighted average water content and observed water content from cosmic-ray sensor. Data points are averaged over 8 hours and depth weighted with equations (5) and (7).

Figure 8. a) Estimate of daily soil water flux using cosmic-ray soil moisture data where positive values are water infiltration into the soil and negative values are evapotranspiration and deep drainage. b) Time series of daily precipitation observed over the footprint. Note that the small positive and negative fluctuations in a) during long dry periods are due to neutron uncertainty, which can be filtered out with additional smoothing of the soil moisture time series.

 doi:10.2136/vzj2012.0046

Tables

Table 1. Summary of chemical composition of soil collected from the Santa Rita Experimental Range study site.

Compound	Weight Percent
SiO_2	60.11
Al_2O_3	9.72
Fe_2O_3	2.77
MnO	0.08
MgO	1.70
CaO	10.60
Na_2O	1.61
K_2O	2.75
TiO_2	0.39
P_2O_5	0.10
Cr_2O_3	0.01
V_2O_5	0.01
CO_2	6.75
H_20^+	2.50 (0.458) †
Total	99.08

† Value in parenthesis is 1 standard error of the mean of three random samples collected within the footprint.

 doi:10.2136/vzj2012.0046

Table 2. Summary of five volumetric calibration datasets at SRER.

Sample Date	**10/10/2010**	**1/6/2011**	**9/11/2011**	**12/15/2011**	**2/18/2012**
Number of Samples Used in Dataset	36	104	108	108	96
Bulk Density (0-30 cm, g cm^{-3}) †	1.40 (0.018)	1.46 (0.016)	1.44 (0.017)	1.52 (0.012)	1.47 (0.016)
Soil Moisture (0-30 cm, m^3 m^{-3}) †	0.0511 (0.0023)	0.0629 (0.0022)	0.0948 (0.0030)	0.153 (0.0026)	0.0818 (0.0019)
Depth Weighted Soil Moisture Using Equations (5) and (7) (m^3 m^{-3})	0.0517	0.0682	0.1046	0.1420	0.0810
Effective Sensor Depth Using Equation (5) (cm)	35	31	27	21	29
Intensity Corrected Fast Neutron Count, Level 2 Data from COSMOS Website (counts hr^{-1}) ‡	2795 (22)	2672 (22)	2230 (8)	2137 (12)	2528 (15)
Intensity and Water Vapor Corrected Fast Neutron Count using equation (2) (counts hr^{-1}) ‡	2833 (25)	2672 (23)	2301 (3)	2173 (13)	2528 (15)

† Values in parenthesis are 1 standard error of the mean.

‡ Values in parenthesis are 1 standard error of the mean, where the count rates have been averaged between 10 AM and 4PM local time when the calibration samples were collected. All datasets are corrected for incoming neutron intensity and water vapor according to the conditions on 1 January 2011.

Raw neutron datasets are available at http://cosmos.hwr.arizona.edu/Probes/StationDat/011/index.php and calibration datasets are available at http://cosmos.hwr.arizona.edu/Probes/StationDat/011/calib.php

doi:10.2136/vzj2012.0046

Table 3. Summary of volumetric calibration datasets and uncertainty between various datasets.

Calibration Sample Date	**10/10/2010**	**1/6/2011**	**9/11/2011**	**12/15/2011**	**2/18/2012**	**All Five Calibration Datasets**
Depth Weighted Soil Moisture (m^3 m^{-3})	0.0517	0.0682	0.1046	0.1420	0.0810	-
Computed N_0 (counts hr^{-1}) †	3311.9	3291.7	3116.2	3172.6	3228.9	3187.0
Matrix of Soil Moisture Deviation Between Calibration Datasets (m^3 m^{-3})						
10/10/2010	-	0.0018	0.0166	0.0120	0.0072	0.0108
1/6/2011	-0.0021	-	0.0172	0.0118	0.0063	0.0104
9/11/2011	-0.0295	-0.0263	-	-0.0081	-0.0165	-0.0102
12/15/2011	-0.0259	-0.0220	0.0097	-	-0.0101	-0.0025
2/18/2012	-0.0098	-0.0074	0.0126	0.0064	-	0.0048
Computed Uncertainty of Calibration Datasets						
Average Absolute Deviation Between Calibration Datasets (m^3 m^{-3})	0.0168	0.0144	0.0140	0.0096	0.0101	0.0097
Percent Error of Observed Soil Moisture	32.5	21.0	13.4	6.7	12.4	19.4% at 0.05 m^3 m^{-3} and 6.5% at 0.15 m^3 m^{-3}

† Values computed with equation (1) using depth weighted soil moisture and intensity and water vapor corrected neutron counts summarized in Table 3.

 doi:10.2136/vzj2012.0046

Table 4. Summary of cosmic-ray sensor footprint water balance between 26 June 2011 and 5 January 2012 calculated with daily averages of rainfall and changes in cosmic-ray soil moisture.

Rainfall (mm)	218.7
Infiltration (mm)	181.8
Evapotranspiration and deep drainage (mm)	168.7
Storage (mm)	13.1
Interception and runoff (mm)	36.9

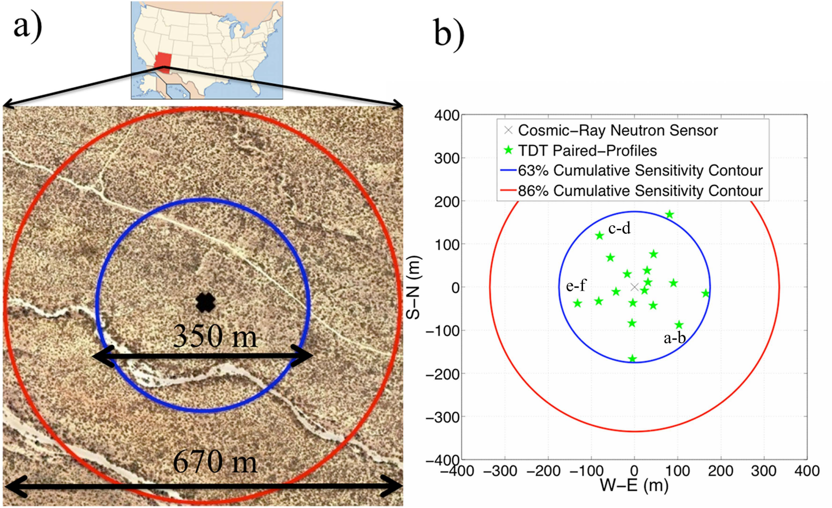
a)
350 m
670 m
b)
Cosmic–Ray Neutron Sensor
TDT Paired–Profiles
63% Cumulative Sensitivity Contour
86% Cumulative Sensitivity Contour
c-d
e-f
a-b
S–N (m)
W–E (m)
400
300
200
100
0
−100
−200
−300
−400

Vadose Zone Journal Accepted Paper, posted 08/20/2012 doi:10.2136/vzj2012.0046

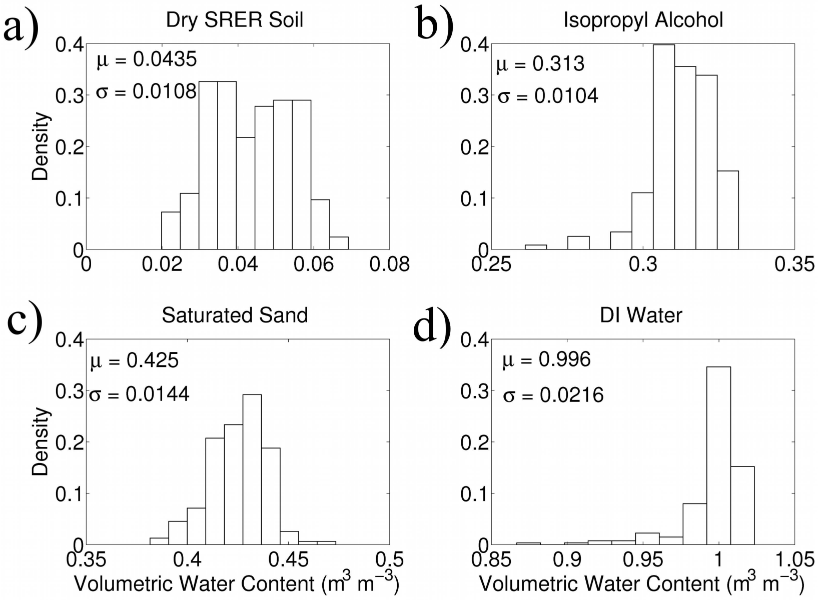

Vadose Zone Journal Accepted Paper, posted 08/21/2012 doi:10.2136/vzj2012.0046

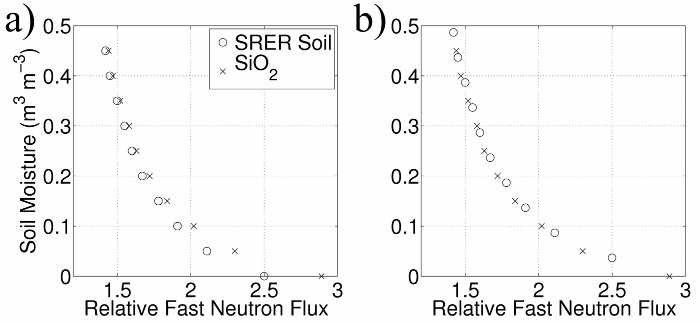

doi:10.2136/vzj2012.0046

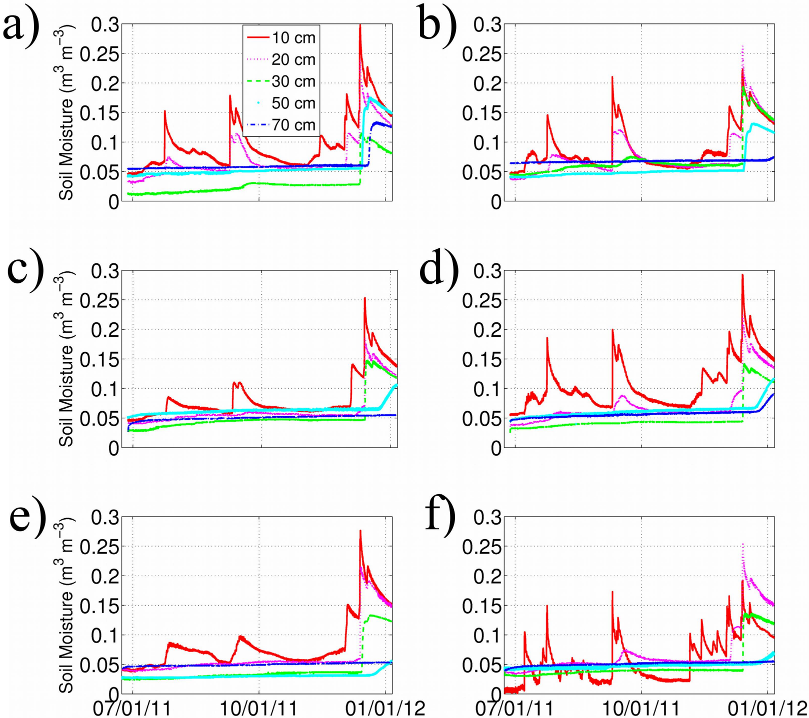

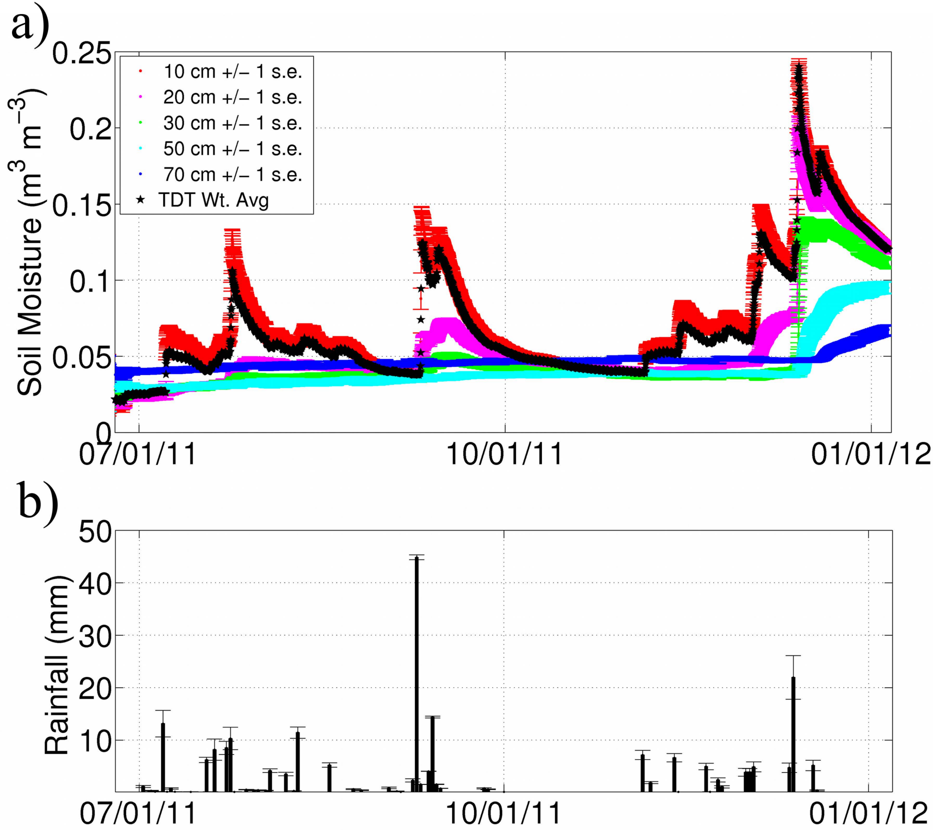
a)
0.25
0.2
0.15
0.1
0.05
0
Soil Moisture (m^3 m^-3)
10 cm +/− 1 s.e.
20 cm +/− 1 s.e.
30 cm +/− 1 s.e.
50 cm +/− 1 s.e.
70 cm +/− 1 s.e.
TDT Wt. Avg
07/01/11
10/01/11
01/01/12
b)
50
40
30
20
10
Rainfall (mm)
07/01/11
10/01/11
01/01/12

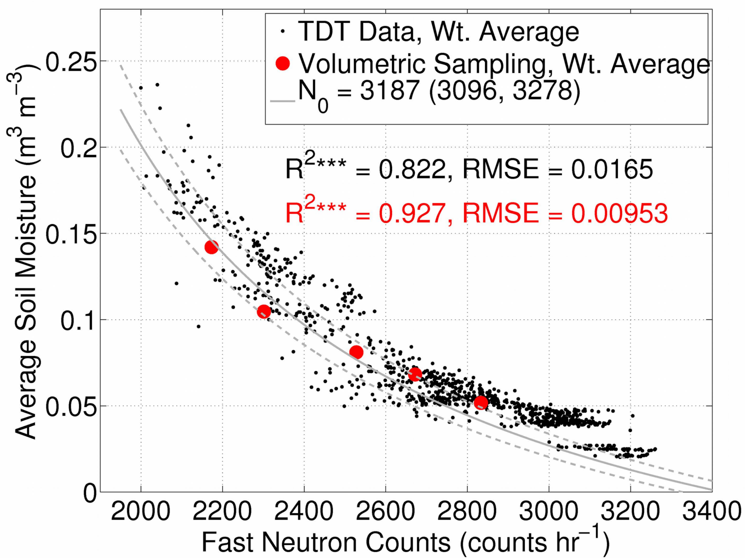

TDT Data, Wt. Average
Volumetric Sampling, Wt. Average
N_0 = 3187 (3096, 3278)
R^{2***} = 0.822, RMSE = 0.0165
R^{2***} = 0.927, RMSE = 0.00953
Average Soil Moisture (m^3 m^{-3})
0.25
0.2
0.15
0.1
0.05
0
2000
2200
2400
2600
2800
3000
3200
3400
Fast Neutron Counts (counts hr^{-1})

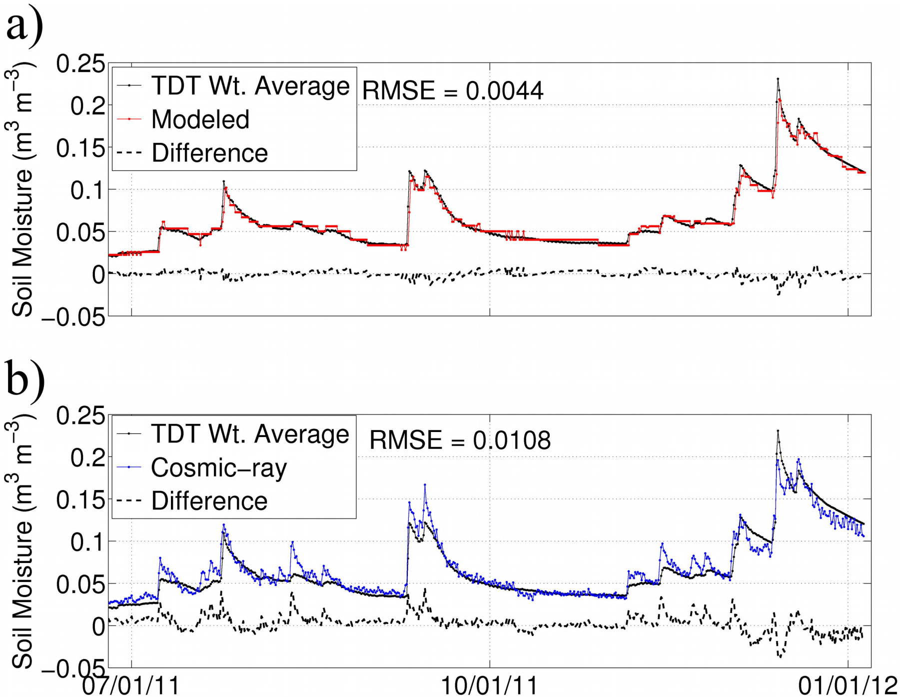
a)
TDT Wt. Average
Modeled
Difference
RMSE = 0.0044
Soil Moisture (m^3 m^-3)
0.25
0.2
0.15
0.1
0.05
0
−0.05
b)
TDT Wt. Average
Cosmic−ray
Difference
RMSE = 0.0108
Soil Moisture (m^3 m^-3)
07/01/11
10/01/11
01/01/12

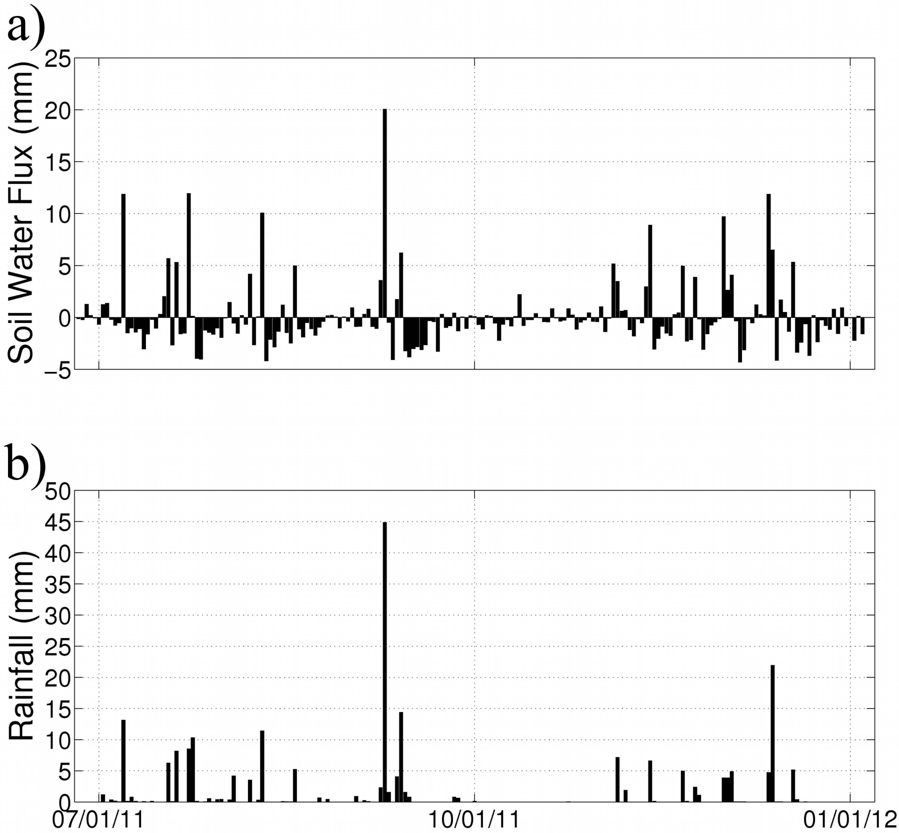
a)
Soil Water Flux (mm)
25
20
15
10
5
0
−5
b)
Rainfall (mm)
50
45
40
35
30
25
20
15
10
5
0
07/01/11
10/01/11
01/01/12